Available online at www.sciencedirect.com
SCIENCE DIRECT®
Journal of Organometallic Chemistry 690 (2005) 1033–1043
Journal of Organometallic Chemistry
www.elsevier.com/locate/jorganchem

Reaction of the heterometallic cluster $Os_3Ru(\mu\text{-}H)_2(CO)_{13}$ with diphenylphosphine: phosphido-bridged tetrahedral and butterfly clusters

Leonard Joachim Pereira, Kwai Sum Chan, Weng Kee Leong *

Department of Chemistry, National University of Singapore, Kent Ridge, Singapore 119260, Singapore

Received 20 October 2004; accepted 9 November 2004

Abstract

TMNO-activated reaction of the heteronuclear cluster $Os_3Ru(\mu\text{-}H)_2(CO)_{13}$ (**1**) with diphenylphosphine afforded the novel phosphido-bridged clusters $Os_3Ru(\mu\text{-}PPh_2)(\mu\text{-}H)_3(CO)_{11}$ (**2**), $Os_3Ru(\mu\text{-}PPh_2)_2(\mu\text{-}H)_2(CO)_{10}$ (**3**), $Os_3Ru(\mu\text{-}PPh_2)_2(\mu\text{-}H)_4(CO)_9$ (**4**), and $Os_3Ru(\mu\text{-}PPh_2)(\mu\text{-}H)_3(CO)_{11}(PPh_2H)$ (**5**). The formation of **2**–**5** proceeded via P–H bond cleavage in the adduct $Os_3Ru(\mu\text{-}H)_2(CO)_{12}(PPh_2H)$ (**6**). Reaction of **2** with PPh_3 afforded the adduct $Os_3Ru(\mu\text{-}PPh_2)(\mu\text{-}H)_3(CO)_{11}(PPh_3)$ (**7**) and the substituted derivative $Os_3Ru(\mu\text{-}PPh_2)(\mu\text{-}H)_3(CO)_{10}(PPh_3)$ (**8**).

Keywords: Osmium; Ruthenium; Clusters; Phosphido; Heteronuclear

1. Introduction

Heteronuclear clusters are of interest because they can display synergistic interactions among the differing metal atoms, giving rise to interesting new chemistry [1]. In the case where there are two metals from the same triad, one may expect that the chemistry at the two types of metal centres will be similar, perhaps differing mainly in their relative reactivity. These clusters provide an opportunity to investigate any subtle effects that may be present in such juxtaposition of two similar metals.

We have recently reported a high-yield synthesis of the hetero group 8 tetranuclear cluster $Os_3Ru(\mu\text{-}H)_2(CO)_{13}$ (**1**), including its reactivity with PPh_3 [2]. The chemistry of this cluster has otherwise been little investigated; so far, only its synthesis and structure [3], and its employment as a catalyst precursor supported on alumina for a number of catalytic reactions including alkene isomerisation and hydrogenation [4], and CO hydrogenation [5], have been reported. A much larger volume of work exists on the closely related clusters $FeRu_3(\mu\text{-}H)_2(CO)_{13}$ [6], and $FeOs_3(\mu\text{-}H)_2(CO)_{13}$ [7]. Cluster **1** is of interest to us because it is envisaged that the ruthenium vertex is expected to be more reactive than the osmium vertices. Thus, we expect that this cluster will react under relatively milder conditions compared to typical homonuclear osmium clusters, but yet should be less susceptible to fragmentation of the cluster core compared to typical homonuclear ruthenium clusters. In this report, we describe our investigations into its reaction with diphenylphosphine, which gives rise to a number of phosphido-bridged tetranuclear clusters.

2. Results and discussion

The reaction of **1** with PPh_2H under TMNO (trimethylamine-*N*-oxide) activation gave, upon chromatographic separation, the new clusters $Os_3Ru(\mu\text{-}PPh_2)$-(μ-

* Corresponding author. Tel.: +65 68745131; fax: +65 67791691.
E-mail address: chmlwk@nus.edu.sg (W.K. Leong).

0022-328X/$ - see front matter © 2004 Elsevier B.V. All rights reserved.
doi:10.1016/j.jorganchem.2004.11.014

$H)_3(CO)_{11}$ (**2**), $Os_3Ru(\mu\text{-}PPh_2)_2(\mu\text{-}H)_2(CO)_{10}$ (**3**), $Os_3Ru(\mu\text{-}PPh_2)_2(\mu\text{-}H)_4(CO)_9$ (**4**), and $Os_3Ru(\mu\text{-}PPh_2)(\mu\text{-}H)_3(CO)_{11}(PPh_2H)$ (**5**). All these products have been completely characterised by spectroscopic, elemental and single crystal X-ray crystallographic analyses. ORTEP plots showing the atomic numbering schemes, together with selected bond parameters, are given in the figures below (Figs. 1–4).

Clusters **2**–**4** are formally 60-electron species, while **5** is a 62-electron species; accordingly, the metal cores adopt closed tetrahedral and "butterfly" geometries, respectively. In **5**, the phosphido bridge is across an open Ru···Os edge and hence the angle at the phosphorus atom is correspondingly large (~106° compared to ~75° for **2**–**4**); such a phosphido bridge is rather uncommon [8]. With the exception of **4**, in which the hydrides were located from a low angle difference map, the hydride locations were placed by potential energy calculations using the program XHYDEX [9]. It is worth noting that the hydrides did not always bridge the longer metal–metal edges. The sum of the M–C and C–O distances vary between 3.01 and 3.10 Å [10], while the M–C–O angles range from 170° to 180°; typical values for terminal carbonyls. The sole exception is the presence of a bridging carbonyl (CO(31)) in **3**.

The crystals of both **3** and **4** exhibited disorder of the metal framework. In **3**, the disorder was modelled with the ruthenium on three alternative positions (M(2), M(3) and M(4), where M = Os or Ru), with ruthenium occupancies refined to about 0.3, 0.2 and 0.5, respectively. This disorder model is in agreement with the existence of isomers in solution (see below). In **4**, there is disorder of the ruthenium about two alternative sites, leading to the crystallographic mirror symmetry observed in the structure. The structures of **3** and **4** are very similar; the two phosphorus atoms are almost coplanar with an Os_2Ru face, and hence their structures can be described as an Os_2RuP_2 raft capped by an

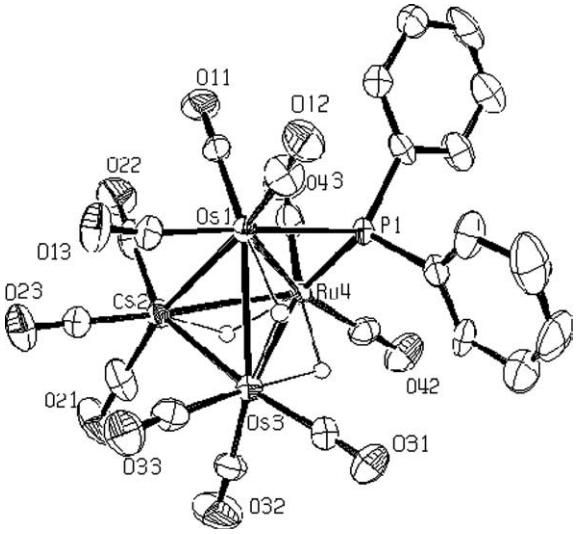

Fig. 1. ORTEP diagram of **2** (50% thermal ellipsoids) with phenyl hydrogens omitted. Os(1)–Os(2) = 3.0145(7) Å; Os(1)–Os(3) = 2.9731(7) Å; Os(1)–Ru(4) = 2.8755(10) Å; Os(2)–Os(3) = 2.7954(7) Å; Os(2)–Ru(4) = 2.7952(11) Å; Os(3)–Ru(4) = 2.9604(11) Å; Os(1)–P(1) = 2.418(3) Å; Ru(4)–P(1) = 2.264(3) Å; Os(1)–P(1)–Ru(4) = 75.69(10)°.

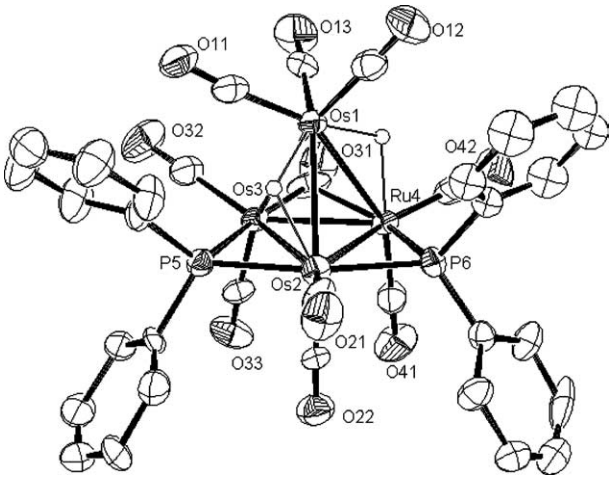

Fig. 2. ORTEP diagram of **3** (50% thermal ellipsoids) with phenyl hydrogens omitted. The ruthenium is modelled as disordered over metal positions Os(2), Os(3) and Ru(4), with occupancies of 0.3, 0.2 and 0.3, respectively. Os(1)–Os(2) = 3.0358(5) Å; Os(1)–Os(3) = 2.8266(5) Å; Os(1)–Ru(4) = 2.9618(6) Å; Os(2)–Os(3) = 2.8686(5) Å; Os(2)–Ru(4) = 2.8344(6) Å; Os(3)–Ru(4) = 2.7377(7) Å; Os(2)–P(5) = 2.352(2) Å; Os(3)–P(5) = 2.364(3) Å; Os(2)–P(6) = 2.364(2) Å; Ru(4)–P(6) = 2.286(2) Å; Os(3)–C(31) = 2.002(11) Å; Ru(4)–C(31) = 2.427(12) Å; Os(2)–P(5)–Os(3) = 74.94(7)°; Os(2)–P(6)–Ru(4) = 75.09(7)°; Os(3)–C(31)–Ru(4) = 75.7(3)°.

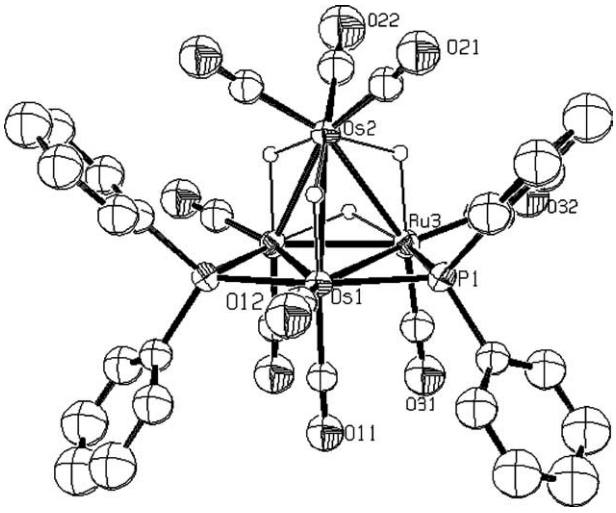

Fig. 3. ORTEP diagram of **4** (50% thermal ellipsoids) with phenyl hydrogens omitted. The ruthenium is modelled as disordered over metal positions Os(3) and Ru(4), with equal occupancies. Os(1)–Os(2) = 3.0416(5) Å; Os(1)–Os(3)/Ru(3) = 2.9003(4) Å; Os(2)–Os(3)/Ru(3) = 3.0276(5) Å; Os(3)–Ru(3) = 2.7478(7) Å; Os(1)–P(1) = 2.3651(17) Å; Os(3)/Ru(3)–P(1) = 2.2903(17) Å; Os(1)–P(1)–Ru(3)/Os(3) = 77.05(5)°.

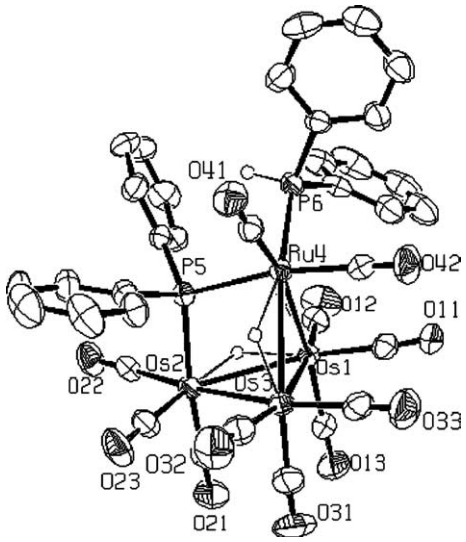

Fig. 4. ORTEP diagram of **5** (50% thermal ellipsoids) with phenyl hydrogens omitted. Os(1)–Os(2) = 3.0053(3) Å; Os(1)–Os(3) = 2.8258(3) Å; Os(1)–Ru(4) = 3.1082(5) Å; Os(2)–Os(3) = 2.9018(3) Å; Os(3)–Ru(4) = 3.0709(5) Å; Os(2)–P(5) = 2.424(2) Å; Ru(4)–P(5) = 2.4147(14) Å; Ru(4)–P(6) = 2.354(2) Å; Os(2)–P(5)–Ru(4) = 105.94(6)°.

$Os(CO)_3$ unit. Their ligand sets differ only by the replacement of one (bridging) carbonyl in **3** by two hydrides in **4**. It appears that the replacement of a carbonyl by two hydrides results in an "expansion" of the metal framework; all the corresponding metal–metal bond lengths are longer in **4** than in **3**, a situation reminiscent of that we have found recently in an osmium–selenium system [11]. There have been a few tetraruthenium clusters containing bridging phosphido ligands reported [12], but none of tetraosmium. The most structurally closely related example to the clusters reported here is the tetraruthenium cluster $Ru_4(\mu\text{-}PPh_2)_2(\mu\text{-}H)_2(CO)_{10}$ [13]; it is essentially isostructural to **3**.

The ^{1}H NMR spectrum of **2** comprised three sets of apparent doublets for the hydrides at −13.04, −19.20 and −21.59 ppm. A ^{1}H COSY, however, showed correlation between the resonance at −19.20 ppm with the other two so that, assuming that the solid-state structure is the same as the solution structure, this resonance can be assigned to H(34) which bridges the Os(3)–Ru(4) edge. Although the hydride positions have been located computationally using the XHYDEX programme [9], nevertheless we believe that it is reasonable to use the so-derived bond parameters to aid in the tentative assignments of the NMR data. Thus, from the X-ray structure, the ∠PMH (M = Ru or Os) for the hydrides are estimated to be 159° for H(24), 79° for H(13) and 87° for H(34). Since the $^2J_{PH}$ will be dependent on this angle, it is reasonable to assign the resonance at −13.04 ppm ($^2J_{PH}$ = 23.9 Hz) to H(24). This leaves the most upfield resonance at −21.59 ppm assignable to H(13), which bridges an Os–Os edge. This is also consistent with earlier observations that the bridging hydride resonance in tetranuclear clusters is shifted increasingly upfield along the series Ru–Ru, Ru–Os and Os–Os [14]. The NMR assignments for **2** are thus as depicted in Fig. 5.

An EXSY spectrum taken at 298 K with a mixing time (τ_m) of 0.5 s showed exchange among all the three resonances. The simplest mechanism involving simultaneous exchange among all three resonances is one that entails movement of the phosphido bridge; all reasonable exchanges involving hydrides only require mutual exchanges between two hydrides. However, an EXSY taken with τ_m = 0.1 s showed absence of the exchange crosspeak between the resonances due to H(24) and H(13). Since the crosspeak amplitudes are a function of the exchange rates [15], this indicates that the exchanges occur with different rates hence ruling out a concerted mechanism.

The $^{31}P\{^1H\}$ and ^{1}H NMR spectra of **3** show that there are two isomers, in about a 7:3 ratio, in solution. This ratio is consistent with the disorder observed in the X-ray crystal structure mentioned above; the disorder over M(3) and M(4) corresponded to enantiomers (with respect to the heavy atoms). The major isomer shows two sets of doublets at about 181.5 and 288.9 ppm in the $^{31}P\{^1H\}$ NMR spectrum, and a −17.90 ppm doublet and a −22.12 ppm doublet of doublets for the hydrides in the ^{1}H NMR spectrum; the minor isomer shows two sets of doublets at about 239.3 and 277.1 ppm in the $^{31}P\{^1H\}$ NMR spectrum, and a −17.23 ppm doublet and a −21.46 ppm doublet of doublets for the hydrides in the ^{1}H NMR spectrum. The P–P and P–H correlations have been confirmed by $^{31}P\{^1H\}$ COSY, and ^{31}P–^{1}H HMBC and selective decoupling, respectively. Assuming that the major isomer has the structure of that in the solid-state X-ray crystallographic study, the structures and NMR assignments for the isomers may tentatively be made as shown in Fig. 5. The two ^{31}P chemical shifts for the proposed structure for the minor isomer are also consistent with the 200–290 ppm range for a phosphido bridge across an Ru–Os edge (compounds **2** and **4**, and the major isomer) compared with the <190 ppm for across an Os–Os edge (for the major isomer and **4**), observed here and in other similar systems [12c,13,16].

The ^{1}H NMR of **4** exhibits four sets of hydride resonances, at −11.40, −19.38, −19.72 and −23.03 ppm; the $^{31}P\{^1H\}$ NMR shows two resonances at 228.5 and 164.3 ppm. These have been tentatively assigned (Fig. 5) with the aid of ^{31}P–^{1}H HMBC, ^{1}H NOESY and selective decoupling experiments. Thus, the ^{1}H resonance at −11.40 ppm is coupled to both ^{31}P resonances, which identifies it as the resonance for H(34). The −19.38 and −19.72 ppm ^{1}H resonances are coupled to the ^{31}P resonances at 164.3 and 228.5 ppm, respectively.

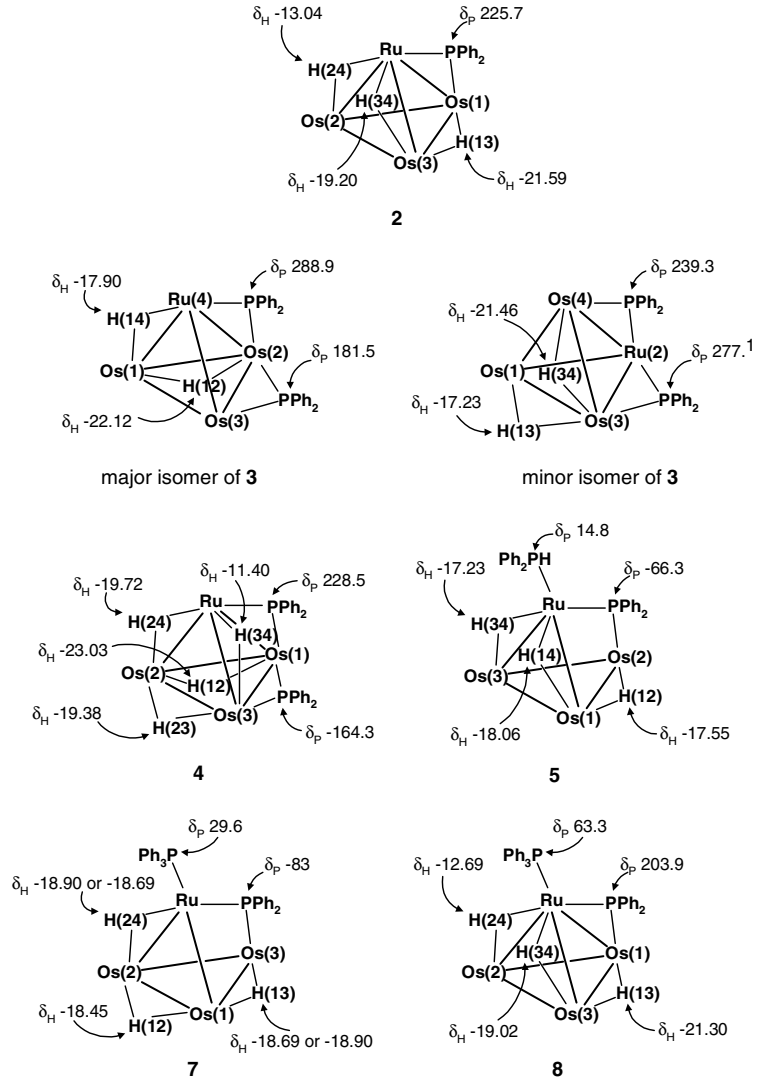

Fig. 5. Tentative NMR assignments and proposed solution structures (carbonyls omitted) for **2**, **3**, **4**, **5**, **7** and **8**.

Furthermore, the NOESY showed crosspeaks between all the ^{1}H resonances except for that between the −11.40 and −23.03 ppm resonances, suggesting that the latter resonance should be assigned to H(12). The HMBC actually shows crosspeaks between the $\delta_H = -23.03$ ppm resonance with both ^{31}P resonances, implying that there is a very small $^2J_{PH}$ associated; this is consistent with the X-ray structure which shows that both ∠POs(1)H(12) is ∼90°. In line with the expected relationship of the $^2J_{PH}$ with ∠PMH [17], the larger $^2J_{HP}$ of 21 and 18 Hz for the ^{1}H resonance at −11.40 ppm are associated with the larger ∠PMH(12) of ∼158°.

The ^{1}H NMR spectrum of **5** at room temperature exhibits three broad resonances in the metal hydride region; at 253 K, these resolved into a set of doublet at −17.55 ppm and two sets of doublet of doublets at −17.23 and −18.06 ppm. Thus, the hydrides in **5** are more fluxional than those in the other compounds. The ^{31}P{^{1}H} NMR spectrum showed resonances at 14.8 and −66.3 ppm. These have also been tentatively assigned with the aid of ^{31}P–^{1}H HMBC and selective decoupling experiments (Fig. 5). The ^{31}P assignments are readily made based on the large $^1J_{PH}$ observed for the $\delta_P = 14.8$ ppm resonance which is thus assignable to P(6). The ^{1}H doublet at −17.56 ppm can be assigned to H(12); the large ∠PMH of ∼168° for P(6)Ru(4)H(34), compared to between 70° and 84° for the others, suggests that the largest $^2J_{PH}$ of 36.3 Hz should be assigned to that between P(6) and H(34) (corresponding to resonances $\delta_P = 14.8$ ppm and $\delta_H = -17.23$ ppm, respectively). The ^{1}H resonance for the P–H is observed as a doublet of doublets at 4.03 ppm.

The reaction was found to afford a slight, and probably insignificant, difference in product distributions when either excess or 2.0 equivalents of the phosphine was employed. More importantly, however, was the observation that a limiting IR spectrum was obtained within 5 min. This IR spectrum (Fig. 6) is similar in

pattern to that of the previously reported PPh_3 derivatives of **1**, viz., $RuOs_3(\mu\text{-}H)_2(CO)_{12}(PPh_3)$ [18], suggesting that it is $RuOs_3(\mu\text{-}H)_2(CO)_{12}(PPh_2H)$ (**6a**). Weaker IR absorption peaks, similar in position to those of the disubstituted derivatives of **1**, have also been noticed in the same spectrum of the reaction mixture, thus suggesting the formation of $RuOs_3(\mu\text{–}H)_2(CO)_{11}(PPh_2H)_2$ (**6b**), as well [19]. The room temperature $^{31}P\{^1H\}$ NMR spectrum of this sample shows a number resonances lying between δ 25 to −80, with the most prominent being a resonance at δ 21.8 ppm, which is assignable to **6a**, as well as resonances assignable to the free phosphine at δ−40.3 ppm, and to **5**. The absence of resonances downfield of 150 ppm clearly indicates that no bridging phosphido ligands have yet been formed. Likewise, the ^1H NMR spectrum in the high field region shows two very prominent sets of doublets at δ−16.7 ppm ($^2J_{PH}$ = 15.7 Hz) and at δ−16.9 ppm ($^2J_{PH}$ = 12.4 Hz), which are assignable to **6a**.

The tentative identification of the initial reaction product as primarily **6a** thus suggests that clusters **2**–**5** resulted from further transformation of **6a**. Indeed, an IR spectrum taken immediately after solvent removal from the reaction mixture indicated that **6a** has already largely been transformed. After the filtration through silica gel to remove unreacted TMNO and trimethylamine, the IR spectrum showed peaks due to **2**–**5**. In analogy with, for example, $Ru_3(CO)_{11}(PPh_2H)$ [20], it is probable that **6a** afforded **2** via loss of a CO and insertion into the P–H bond. Cluster **2** itself is thermally stable in solution; its NMR spectrum remaining unchanged after more than two years. In contrast, a ^1H NMR spectrum of **5** recorded after standing the solution for a month showed the coexistence of **2**–**5**. Five months later, only peaks due to **2** (10%), **3** (30%) and **4** (70%) were seen; decomposition was complete. A solution of **4** only partly decomposes, even on long standing (at least a year), to **2** and **3**; the relative proportions of clusters **2**, **3** and **4** obtained being the same as in the case for **5**. We believe that the reaction of **2** with an excess of PPh_2H gave rise to the adduct **5** via metal–metal bond cleavage; this was verified by reacting a CH_2Cl_2 solution of **2** with PPh_2H a room temperature which gave **5** immediately, as observed by IR spectroscopy. It is also possible that the formation of **3** to **5** proceeded from the disubstituted derivative **6b**; this has analogies in the trinuclear analogues $M_3(CO)_{10}(PPh_2H)_2$ (M = Ru, Os), which form the phosphido species $M_3(\mu\text{-}H)_2(\mu\text{-}PPh)_2(CO)_8$ at elevated temperatures [21]. We are, however, unable to assess the precise contributions of **6a** and **6b** towards the final product distribution. At the present time, we can summarise our picture of the reaction scheme from **6a** as shown in Scheme 1.

We have further investigated the adduct formation of **2** with the tertiary phosphine PPh_3. Thus, on stirring a solution of **2** with PPh_3 at room temperature, a limiting IR spectrum was obtained within 10 min. An attempt at chromatographic separation was only partially successful as it yielded bands which were mixtures of similar composition, suggesting interconversion between at least two species. Fractional crystallization from a dichloromethane/hexane mixture afforded orange crystals of $RuOs_3(\mu\text{-}H)_3(CO)_{11}(\mu\text{-}PPh_2)(PPh_3)$ (**7**), and dark red crystals of $RuOs_3(\mu\text{-}H)_3(CO)_{10}(\mu\text{-}PPh_2)(PPh_3)$ (**8**).

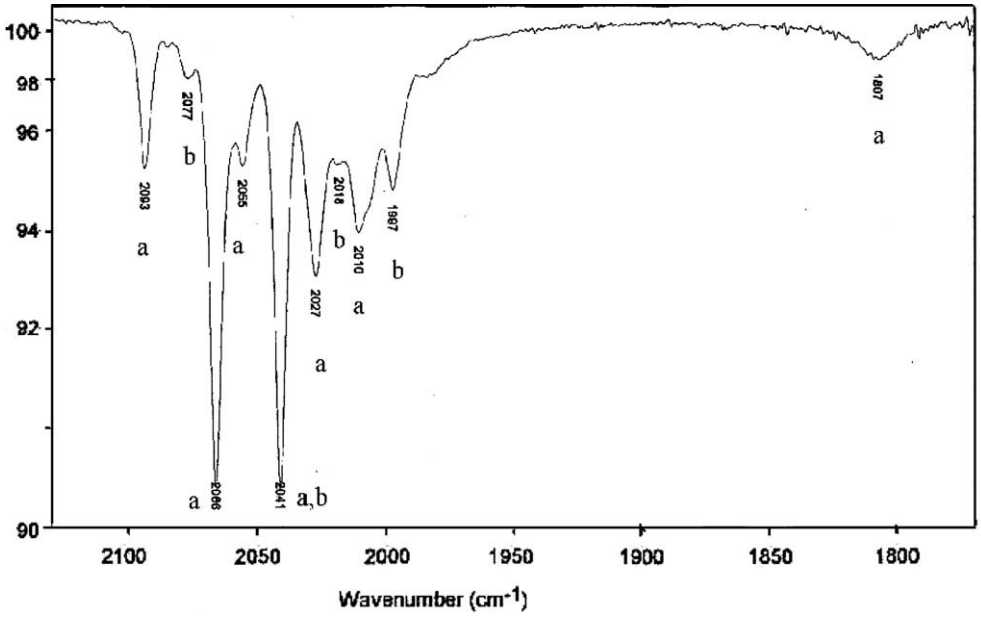

Fig. 6. IR spectrum (in hexane) of the reaction mixture resulting from the addition of PPh_2H to **1**. Peaks labelled **a** are assignable to $RuOs_3(\mu\text{-}H)_2(CO)_{12}(PPh_2PH)$, **6a**, and those labelled b are assignable to $RuOs_3(\mu\text{-}H)_2(CO)_{11}(PPh_2PH)_2$, **6b**.

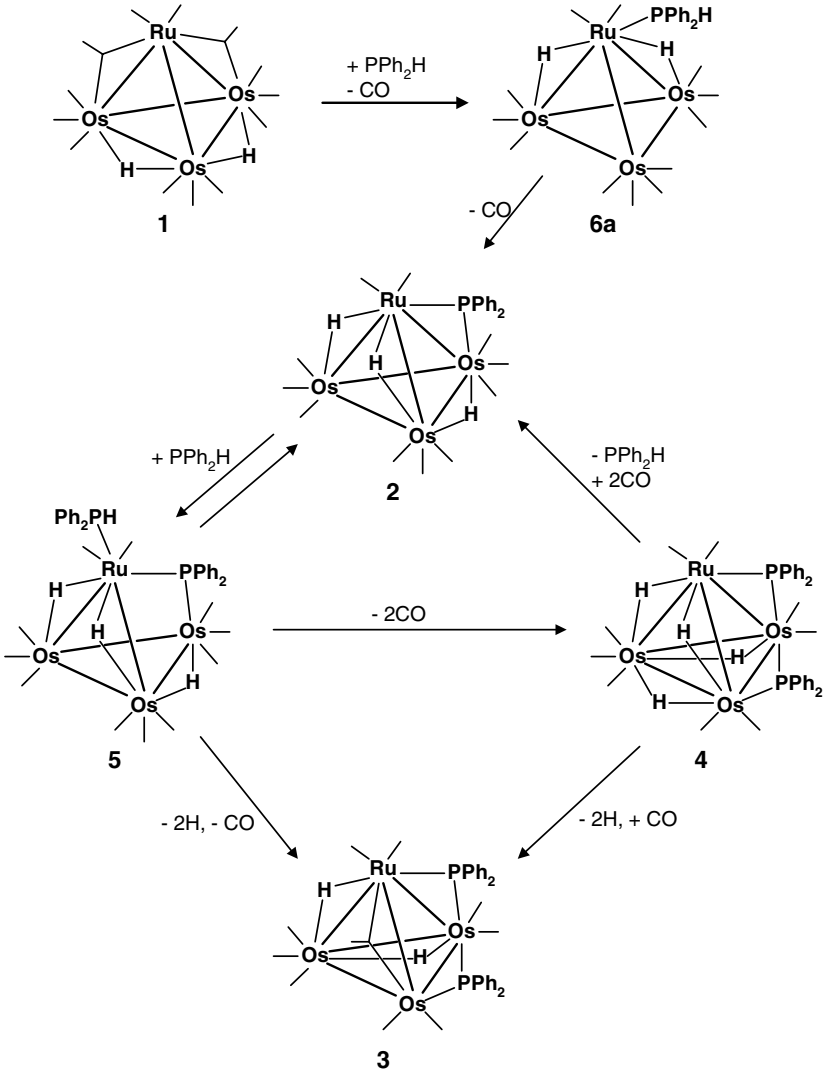

Scheme 1.

These have been characterised completely, including single crystal X-ray crystallographic studies; the ORTEP plots showing the atomic numbering schemes, together with selected bond parameters, are given in the figures below (Figs. 7 and 8, respectively).

There are two crystallographically independent molecules in the asymmetric unit of **8**; with fairly similar bond parameters. The molecules consisted of a distorted tetrahedron with a terminal PPh_3 ligand attached to the Ru vertex and a phosphido bridge across a Ru–Os edge. No analogous structure with a terminal PPh_2H ligand was identified in the reaction with Ph_2PH, presumably because of the ease with which the P–H bond is cleaved. Its $^{31}P\{^1H\}$ resonances at 63.3 and 203.9 ppm may be assigned to the terminal PPh_3 and the bridging PPh_2, respectively. Selective decoupling and ^{31}P–^1H HMBC correlated the two doublet of doublets at −12.69 and −19.02 ppm in the ^1H NMR spectrum with both the ^{31}P resonances, and the doublet at −21.30 ppm with the lower field ^{31}P resonance. The H–M–P angles observed in the solid-state structure, even though the hydrides are placed by potential energy calculations [9], can be correlated with the observed $^2J_{PH}$ values; the ∠H(24)Ru(4)P(1) of ∼161° was expected to give rise to the largest coupling constant (30.5 Hz), compared with ∠H(24)Ru(4)P(2) (∼90°), and two similar angles, viz., ∠H(34)Ru(4)P(1) and ∠H(34)Ru(4)P(2) (∼82° and ∼81°, respectively). This allowed assignment of the δ_H −12.69 ppm to H(24); the other $^2J_{PH}$ value of 9.1 Hz for this resonance, and a doublet of doublets with nearly equal coupling constants (10 Hz) for H(34), are also consistent with this. Cluster **8** is best viewed as a PPh_3 substituted derivative of **2**; their ^1H and $^{31}P\{^1H\}$ chemical shifts are surprisingly very similar despite the replacement of one carbonyl in **2** with a PPh_3 in **8** (Fig. 5). The structural parameters for **2** and **8** are also similar (Table 1), and one interesting feature is that the longest metal–metal bond edge in both structures

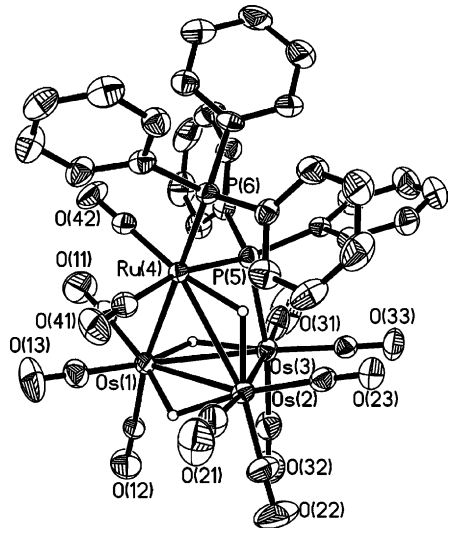

Fig. 7. ORTEP diagram of **7** (50% thermal ellipsoids) with phenyl hydrogens omitted. Ru(4)–Os(1) = 2.8851(6) Å; Ru(4)–Os(2) = 3.0744(6) Å; Ru(4)···Os(3) = 3.826(6) Å; Os(1)–Os(2) = 2.9701(4) Å; Os(1)–Os(3) = 3.0357(4) Å; Os(2)–Os(3) = 2.8938(4) Å; Ru(4)–P(5) = 2.4121(17) Å; Os(3)–P(5) = 2.4319(17) Å; Ru(4)–P(6) = 2.3892(17) Å; Ru(4)–P(5)–Os(3) = 104.36(6)°; P(5)–Ru(4)–P(6) = 99.94(6)°.

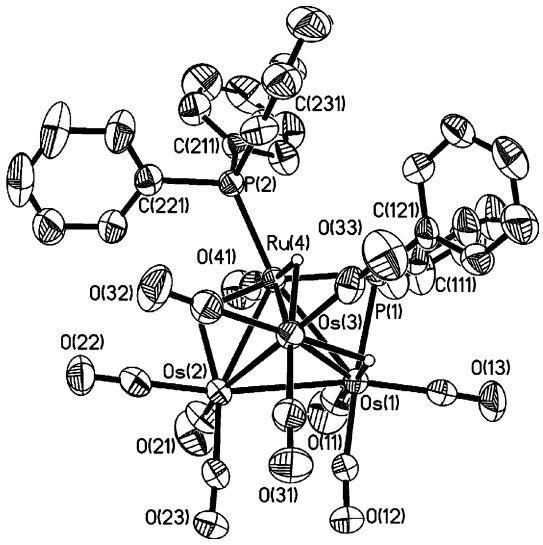

Fig. 8. ORTEP diagram of molecule A of **8** (50% thermal ellipsoids) with phenyl hydrogens omitted. Molecule A: Ru(4)–Os(1) = 2.8629(6) Å; Ru(4)–Os(2) = 2.8026(7) Å; Ru(4)–Os(3) = 2.9664(7) Å; Os(1)–Os(2) = 3.0015(4) Å; Os(1)–Os(3) = 2.9869(5) Å; Os(2)–Os(3) = 2.7987(5) Å; Ru(4)–P(1) = 2.281(2) Å; Os(1)–P(1) = 2.459(2) Å; Ru(4)–P(2) = 2.313(2) Å; Ru(4)–P(1)–Os(1) = 74.20(6)°; P(1)–Ru(4)–P(2) = 110.16(8)°. Molecule B: Ru(4)–Os(1) = 2.8694(7) Å; Ru(4)–Os(2) = 2.7709(7) Å; Ru(4)–Os(3) = 2.9842(7) Å; Os(1)–Os(2) = 3.0260(4) Å; Os(1)–Os(3) = 2.9789(4) Å; Os(2)–Os(3) = 2.8005(4) Å; Ru(4)–P(1) = 2.276(2) Å; Os(1)–P(1) = 2.456(2) Å; Ru(4)–P(2) = 2.312(2) Å; Ru(4)–P(1)–Os(1) = 74.54(6)°; P(1)–Ru(4)–P(2) = 106.74(8)°

is not bridged by a hydride. However, unlike **2**, the hydrides in **8** are not fluxional; no exchange crosspeaks were observed in the ^{1}H EXSY spectrum taken at 243 K, and the resonances remained well-resolved between 223 and 300 K. Such dependence of hydride fluxionality on the properties of the other ligands has been observed by others [22].

Table 1
Comparison of selected bond lengths (Å) and angles (°) for **2** and **8**

Bond parameter	**2**	**8**	
		Molecule A	Molecule B
Ru(4)–Os(1)	2.8755(10)	2.8629(6)	2.8694(7)
Ru(4)–Os(2)	2.7952(11)	2.8026(7)	2.7709(7)
Ru(4)–Os(3)	2.9604(11)	2.9664(7)	2.9842(7)
Os(1)–Os(2)	3.0145(7)	3.0015(4)	3.0260(4)
Os(1)–Os(3)	2.9731(7)	2.9869(5)	2.9789(4)
Os(2)–Os(3)	2.7954(7)	2.7987(5)	2.8005(4)
Ru(4)–P(1)	2.264(3)	2.281(2)	2.276(2)
Os(1)–P(1)	2.418(3)	2.459(2)	2.456(2)
Ru(4)–P(1)–Os(1)	75.69(10)	74.20(6)	74.54(6)

Cluster **7**, like **5**, has a phosphido-bridged butterfly structure, with the terminal PPh_2H ligand replaced by a PPh_3ligand; they differ in the position of one of the hydrides though. Assignments for the ^{1}H and $^{31}P\{^{1}H\}$ NMR spectra of **7** were complicated by the observation that solutions of **7** were invariably found as a mixture with **2** and **8**. Three doublets for the hydrides were observed at −18.45, −18.69 and −18.90 ppm. A ^{31}P–^{1}H HMBC correlated the latter two resonances with the broad $^{31}P\{^{1}H\}$ resonance at −83 ppm, which in analogy to **5**, is assigned to the phosphido bridge. With the assumption that the solid-state structure persisted in solution, the tentative assignments are as given in Fig. 5; it was not possible to assign the ^{1}H resonances at −18.69 and −18.90 ppm unambiguously. As in **5**, the hydrides in **7** are fluxional; the resonances coalesced completely at about 280 K and an EXSY at 243 K showed that all three hydrides were in mutual exchange.

3. Conclusions

The reaction of the heteronuclear cluster **1** with Ph_2PH thus appears to lead initially to the substitution products **6a** and **6b**. These are unstable and decomposed during work-up to a number of species, viz., the phosphido bridged clusters **2**–**5**. Among them are two which contain a relatively rare phosphido bridge across the wingtips of a butterfly core. The solution NMR data of the new clusters support the notion that the solid state structures persist in solution, although some exhibit fluxionality of the hydrides. The reactivity of this class of clusters is basically dictated by the more reactive ruthenium centre; thus the phosphido bridges an Ru–Os edge in almost all the species, and nucleophilic attack in **2** occurs initially at the ruthenium vertex. We are currently examining the reactivity of these heteronuclear clusters with other substrates.

4. Experimental

4.1. General procedures

All reactions and manipulations were carried out under nitrogen by using standard Schlenk techniques. Solvents were purified, dried, distilled, and stored under nitrogen prior to use. 1D NMR spectra were recorded on a Bruker ACF-300 FT NMR spectrometer while 2D NMR spectra were recorded on a Bruker AMX500 NMR spectrometer, as $CDCl_3$ solutions. EXSY spectra were recorded with a mixing time of 0.5s unless otherwise stated. Mass spectra were obtained on a Finnigan MAT95XL-T spectrometer in an *m*-nitrobenzyl alcohol matrix. Microanalyses were carried out by the microanalytical laboratory at the National University of Singapore. The preparation of cluster **1** appears in our earlier report [2]; diphenylphosphine was prepared according to the literature method [23]. All other reagents were from commercial sources and used as supplied.

4.2. Reaction of *1* with diphenylphosphine

A solution of diphenylphosphine in hexane (1.5 mL, 57.5 mmol dm^{-3}) was added to a solution of **1** (87.0 mg, 83 μmol) in dichloromethane (90 mL), which was maintained at −78 °C in an acetone/dry ice bath. $Me_3NO.2H_2O$ (10.6 mg, 95 μmol) in acetonitrile (40 mL) was added dropwise into the mixture. The mixture was stirred for a further 20 min after completion of the addition. This was then filtered through a short column of silica gel, the solvents an volatile material removed in vacuo, and the residue chromatographed on silica gel with hexane/dichloromethane mixtures as eluant to afford an orange-red band of $Os_3Ru(\mu\text{-}PPh_2)(\mu\text{-}H)_3(CO)_{11}$ (**2**) (24 mg, 25%), an orange-pink band of $Os_3Ru(\mu\text{-}PPh_2)_2(\mu\text{-}H)_2(CO)_{10}$ (**3**) (49 mg, 44%), and an orange-brown band of $Os_3Ru(\mu\text{-}PPh_2)_2(\mu\text{-}H)_4(CO)_9$ (**4**) (21 mg, 20%).

A similar reaction with excess diphenylphosphine (2 drops, neat) afforded **2** (40%), another novel compound $Os_3Ru(\mu\text{-}PPh_2)(\mu\text{-}H)_3(CO)_{11}(PPh_2H)$ (**5**) (16%), and **4** (1%).

2: ν_{max}/cm^{-1} (hexane) 2095m, 2066vs, 2050vs, 2039s, 2017mw, 2009mw, 2004ms, 1997mw, 1985m (CO). ^1H NMR δ 7.3–7.8 (m, 10H, aromatic), −13.04 (d, 1H, $^2J_{PH}$ = 23.9 Hz), −19.20 (d, 1H, $^2J_{PH}$ = 11.6 Hz), −21.59 (d, 1H, $^2J_{PH}$ = 8.3 Hz). $^{31}P\{^1H\}$ NMR δ 225.71s. MS: 1167.9 (M^+); calculated for $C_{23}H_{13}O_{11}Os_3PRu$: 1168.8. Anal. Calc. for $C_{23}H_{13}O_{11}Os_3PRu$: C, 23.65; H, 1.12. Found : C, 23.73; H, 1.22%.

3: ν_{max}/cm^{-1} (CH_2Cl_2) 2078ms, 2046vs, 2020vs, 1992m, 1981m, 1966m (CO). ^1H NMR δ 7.2–7.8m (20H, aromatic), −17.23 (d, $^2J_{PH}$ = 10.3 Hz, 25%), −17.90 (d, $^2J_{PH}$ = 11.1 Hz, 75%), −21.46 (dd, $^2J_{PH}$ = 7.4, 7.4 Hz, 25%), −22.12 (dd, $^2J_{PH}$ = 5.8, 5.8 Hz, 75%). $^{31}P\{^1H\}$ NMR δ 288.90d ($^2J_{PP}$ = 161.3 Hz, 75%), 277.13d ($^2J_{PP}$ = 176.6 Hz, 25%), 239.25d ($^2J_{PP}$ = 165.7 Hz, 25%), 181.53d (75%). MS: 1325.0 (M^+); calculated for $C_{34}H_{22}O_{10}Os_3P_2Ru$: 1324.9. Anal. Calc. for $C_{34}H_{22}O_{10}Os_3P_2Ru.1/2C_6H_{14}$: C, 32.50; H, 2.14. Found : C, 32.51; H, 1.83%.

4: ν_{max}/cm^{-1} (hexane) 2117m, 2049vs, 2017m, 2009m, 1974m, 1961ms, 1948m (CO). ^1H NMR δ 7.2–8.0m (20H, aromatic), −11.40 (dd, 1H, $^2J_{PH}$ = 18.0, 21.4 Hz), −19.38 (d, 1H, $^2J_{PH}$ = 6.6 Hz), −19.72 (d, 1H, $^2J_{PH}$ = 8.3 Hz), −23.03 (s, 1H). $^{31}P\{^1H\}$ NMR δ 228.50d ($^2J_{PP}$ = 129 Hz), 164.26d. MS: 1299.0 (M^+); calculated for $C_{33}H_{24}O_9Os_3P_2Ru$: 1298.9. Anal. Calc. for $C_{33}H_{24}O_9Os_3P_2Ru$: C, 30.53; H, 1.85. Found: C, 30.64; H, 1.95%.

5: ν_{max}/cm^{-1} (hexane) 2086m, 2068mw, 2054vs, 2027s, 2007s, 1991mw, 1964w, 1953w (CO). ^1H NMR (253K) δ 7.1–7.8m (20H, aromatic), 4.03 (dd, 1H, $^1J_{PH}$ = 402.5 Hz, $^3J_{PH}$ = 10.2 Hz), −17.23 (dd, $^2J_{HP}$ = 18.2, 36.3 Hz), −17.55 (d, $^2J_{PH}$ = 6.6 Hz), −18.06 (dd, $^2J_{PH}$ = 9.9, 22.3 Hz). $^{31}P\{^1H\}$ NMR δ 14.79d ($^2J_{PP}$ = 7.6 Hz), −66.25d. MS: 1354.7 (M^+); calculated for $C_{35}H_{24}O_{11}Os_3P_2Ru$: 1354.8. Anal. Calc. for $C_{35}H_{24}O_{11}Os_3P_2Ru$: C, 31.04; H, 1.77. Found: C, 30.79; H, 1.87%.

4.3. Reaction of *2* with PPh_3

Cluster **2** (150 mg, 128 μmol), PPh_3 (34 mg, 130 μmol) and dichloromethane (50 mL) were stirred at room temperature in a 3-necked 100 mL rbf. Monitoring by IR spectroscopy indicated that the reaction was complete within 10 min. Chromatographic separation on silica gel using hexane and dichloromethane as eluant yielded three coloured fractions; yellow (27 mg), yellow-red (25 mg) and red (174 mg), in order of elution. IR analysis of the three fractions showed all fractions to be the same mixture of compounds, in about the same relative proportions, comprising **2**, **7** and **8**. Crystallization from a hexane/dichloromethane mixture yielded orange crystalline powder $RuOs_3(\mu\text{-}H)_3(CO)_{11}(\mu\text{-}PPh_2)(PPh_3)$ (**7**), and dark red crystals of $RuOs_3(\mu\text{-}H)_3(CO)_{10}(\mu\text{-}PPh_2)(PPh_3)$ (**8**).

7: ν_{max}/cm^{-1} (hexane) 2091mw, 2085m, 2069m, 2060s, 2050vs, 2039mw, 2025s, 2020m, 2009m, 2005s, 1993w, 1984mw, 1979mw, 1962w, 1953vw, 1944vw (CO). ^1H NMR (233K) δ−18.45d (1H, $^3J_{PH}$ = 4.1 Hz), −18.69d (1H, $^2J_{PH}$ = 10.7 Hz), −18.90d (1H, $^2J_{PH}$ = 13.2 Hz). $^{31}P\{^1H\}$ NMR δ 29.6s (PPh_3), −83br (PPh_2). MS: 1430.9 (M^+); calculated for $C_{41}H_{28}O_{11}Os_3P_2Ru$: 1430.9. Anal. Calc. for $C_{41}H_{28}O_{11}Os_3P_2Ru$: C, 34.43; H, 1.96. Found: C, 34.11; H, 1.92%.

8: ν_{max}/cm^{-1} (hexane) 2084s, 2058vs, 2039vs, 2013s, 2002w, 1994mw, 1983w, 1972w, 1961vw (CO). ^1H

Table 2
Crystal data for **2**, **3**, **4**, **5**, **7** and **8**

Compound	**2**	**3**	**4**	**5**	**7**	**8**
Formula	$C_{23}H_{13}O_{11}Os_3PRu$	$C_{34}H_{22}O_{10}Os_3P_2Ru$	$C_{33}H_{24}O_9Os_3P_2Ru \cdot 1/2CH_2Cl_2$	$C_{35}H_{24}O_{11}Os_3P_2Ru$	$C_{41}H_{28}O_{11}Os_3P_2Ru$	$C_{40}H_{28}O_{10}Os_3P_2Ru \cdot 1/8CH_2Cl_2 \cdot 1/8C_7H_8$
F_w	1167.97	1324.13	1340.60	1354.15	1430.24	1424.37
Temperature (K)	293(2)	223(2)	293(2)	293(2)	233(2)	293(2)
Crystal system	Monoclinic	Orthorhombic	Monoclinic	Monoclinic	Monoclinic	Triclinic
Space group	$P2_1/n$	$P2_12_12_1$	$P2_1/m$	$P2_1/c$	$P2_1/c$	$P\bar{1}$
Unit cell dimensions						
a (Å)	8.3060(1)	12.9224(2)	8.8708(3)	9.1303(1)	14.2111(4)	11.3074(2)
b (Å)	20.4923(3)	14.0768(2)	14.1119(5)	22.6580(1)	12.4835(4)	19.1346(3)
c (Å)	16.8518(2)	20.3403(1)	16.1105(5)	18.7392(1)	23.9748(7)	20.5424(2)
α (°)	90	90	90	90	90	97.926(1)
β (°)	100.083(1)	90	103.940(1)	98.181(1)	96.862(1)	97.231(1)
γ (°)	90	90	90	90	90	93.021(1)
V (Å^3)	2823.93(5)	3700.02(8)	1957.38(11)	3837.21(5)	4222.8	4356.02(11)
No. reflections for unit cell	6044	6294	8192	7117	6007	8192
z	4	4	2	4	4	4
ρ_c (g cm^{-3})	2.747	2.377	2.275	2.344	2.250	2.172
μ (Mo Kα) (mm^{-1})	14.091	10.810	10.282	10.428	9.483	9.205
F(000)	2104	2432	1234	2496	2656	2646
Crystal size (mm × mm × mm)	0.46 × 0.40 × 0.20	0.24 × 0.16 × 0.14	0.34 × 0.15 × 0.14	0.20 × 0.14 × 0.07	0.18 × 0.14 × 0.12	0.38 × 0.28 × 0.08
θ Range (°C)	2.34–29.26	2.00–29.30	2.37–29.34	1.80–29.41	2.10–29.29	2.02–29.35
Reflections collected	21414	24459	12983	25613	27243	34887
Independent reflections (R_{int})	4803 (0.0687)	9127 (0.0471)	4964 (0.0283)	9407 (0.0374)	10318 (0.0460)	20505 (0.0345)
Transmission range	0.154–0.047	0.316–0.206	0.357–0.213	0.357–0.171	0.432–0.353	0.200–0.019
Data/restraints/parameters	4803/0/352	9127/0/380	4964/1/257	9407/6/478	10318/0/532	20505/4/1035
Goodness-of-fit on F^2	1.058	1.083	1.154	1.123	1.097	1.095
Final R indices [$I > 2\sigma(I)$]						
R_1	0.0561	0.0419	0.0342	0.0304	0.0408	0.0425
wR_2	0.1419	0.0675	0.0861	0.0592	0.0646	0.0815
R indices (all data)						
R_1	0.0655	0.0623	0.0460	0.0520	0.0700	0.0725
wR_2	0.1481	0.0758	0.0934	0.0702	0.0740	0.0938
Largest diff. peak and hole (e Å^{-3})	3.197 and −4.718	0.955 and −1.245	1.545 and −1.481	0.892 and −1.413	0.835 and −1.310	1.141 and −1.656

NMR δ 7.0–7.5m (25H, aromatic), −12.69dd (1H, $^2J_{PH}$ = 30.5, 9.1 Hz), −19.02dd (1H, $^2J_{PH}$ = 10.0, 10.0 Hz), −21.30d (1H, $^2J_{PH}$ = 6.6 Hz). $^{31}P\{^1H\}$ NMR δ 63.3s (PPh_3), 203.9s (PPh_2). MS: 1401.8 (M^+); calculated for $C_{40}H_{28}O_{10}Os_3P_2Ru$: 1402.9. Anal. Calc. for $C_{40}H_{28}O_{10}Os_3P_2Ru.1/2CH_2Cl_2$: C, 33.67; H, 2.02. Found: C, 33.58; H, 1.96%. Solvent in the sample has been confirmed by ^1H NMR.

4.4. Crystal structure determinations

Crystals were grown from dichloromethane/hexane solutions and mounted on quartz fibres. X-ray data were collected on a Bruker AXS APEX system, using Mo Kα radiation, with the SMART suite of programs [24]. Data were processed and corrected for Lorentz and polarisation effects with SAINT [25], and for absorption effects with SADABS [26]. Structural solution and refinement were carried out with the SHELXTL suite of programs [27]. Crystal and refinement data are summarised in Table 2.

The structures were solved by direct methods to locate the heavy atoms, followed by difference maps for the light, non-hydrogen atoms. Organic hydrogen atoms were placed in calculated positions and refined with a riding model. The metal hydride positions were calculated with the program XHYDEX [9], except for compounds **4** and **7**, where the hydrides were located from a low angle difference map. The hydrides were given fixed isotropic thermal parameters and generally allowed to ride on one of the osmium atoms that they are attached to. With the exception of those mentioned below involving disordered parts, all non-hydrogen atoms were given anisotropic thermal parameters in the final model.

The crystal of compound **3** exhibited disorder of the ruthenium over three sites. Each of these sites was thus modelled with a partial osmium and ruthenium, given identical anisotropic thermal parameters and positions, with sum of the occupancies of osmium restrained to 2.0. There was also disorder of one of the phenyl rings, which was modelled with two complete rings of half-occupancy, restrained to be regular hexagons and refined with isotropic thermal parameters. The crystal of **4** contained a molecule of CH_2Cl_2 per formula unit of **4**. Both the solvent and the molecule of **4** showed disorder. The solvent disorder was modelled with two alternative sites, and the C–Cl lengths appropriately restrained. The disorder in the molecule of **4** involved one osmium with the ruthenium. The two sites were modelled as containing half of each atom type. The crystal of **8** also contained solvent molecules, which were treated as comprising 1/8 CH_2Cl_2 and 1/8 toluene; the toluene was modelled as disordered about an inversion centre. Appropriate restraints on bond parameters were placed on the solvent molecules.

5. Supplementary material

Crystallographic data (excluding structure factors) for the structures in this paper have been deposited with the Cambridge Crystallographic Data Centre as supplementary publication numbers CCDC 253124–253129. Copies of the data can be obtained, free of charge, on application to CCDC, 12 Union Road, Cambridge CB2 1EZ, UK, (fax: +44 1223 336033 or e-mail: deposit@ccdc.cam.ac.uk).

Acknowledgements

This work was supported by the National University of Singapore (Research Grant No. R143-000-149-112) and one of us (L.J.P.) thank the University for a Research Scholarship.

References

[1] (a) For examples, see S.M. Waterman, N.T. Lucas, M.G. Humphrey, Adv. Organomet. Chem. 46 (2000) 47;
(b) P. Braunstein, L.A. Oro, P.R. Raithby (Eds.), Metal Clusters in Chemistry, vol. 2, Wiley-VCH, Weinheim, 1999;
(c) J. Rose, P. Braunstein, in: G. Wilkinson, F.G.A. Stone, E.W. Abel (Eds.), Comprehensive Organometallic Chemistry II, vol. 10, Pergamon, New York, 1995.
[2] L. Pereira, W.K. Leong, S.Y. Wong, J. Organomet. Chem. 609 (2000) 104.
[3] (a) A.L. Rheingold, B.C. Gates, J.P. Scott, J.R. Budge, J. Organomet. Chem. 331 (1987) 81;
(b) G.A. Foulds, B.F.G. Johnson, J. Lewis, R.M. Sorrell, J. Chem. Soc., Dalton Trans. (1986) 2515;
(c) G.L. Geoffroy, J.R. Fox, E. Burkhardt, H.C. Foley, A.D. Harley, R. Rosen, Inorg. Synth. 21 (1982) 57;
(d) E.W. Burkhardt, G.L. Geoffroy, J. Organomet. Chem. 198 (1980) 179.
[4] (a) J.P. Scott, J.R. Budge, A.L. Rheingold, B.C. Gates, J. Am. Chem. Soc. 109 (1987) 7736;
(b) J.R. Budge, J.P. Scott, B.C. Gates, J. Chem. Soc., Chem. Commun. (1983) 342.
[5] (a) J.R. Budge, B.F. Luecke, J.P. Scott, B.C. Gates, Int. Cong. Catal. Proc. 8th 5 (1984) V89;
(b) J.R. Budge, B.C. Gates, Pan-Pac. Synfuels Conf. 1 (1982) 204.
[6] (a) Some examples B. Bonelli, S. Brait, S. Deabate, E. Garrone, R. Giordano, E. Sappa, F. Verre, J. Cluster Sci. 11 (2000) 307;
(b) M. Castiglioni, R. Giordano, E. Sappa, J. Organomet. Chem. 491 (1995) 111;
(c) L. Huang, A. Choplin, J.M. Basset, U. Siriwardane, S.G. Shore, R. Mathieu, J. Mol. Catal. 56 (1989) 1;
(d) S. Dobos, I. Boszormenyi, J. Mink, L. Guczi, Inorg. Chim. Acta 134 (1987) 203;
(e) T. Venalainen, T.A. Pakkanen, J. Organomet. Chem. 316 (1986) 183;
(f) S. Dobos, A. Beck, S. Nunziante-Cesaro, M. Barbeschi, Inorg. Chim. Acta 130 (1987) 65;
(g) A. Choplin, L. Huang, J.M. Basset, R. Mathieu, U. Siriwardane, S.G. Shore, Organometallics 5 (1986) 1547;
(h) S. Dobos, S. Nunziante-Cesaro, J. Mol. Struct. 142 (1986) 579;

(i) H.C. Foley, G.L. Geoffroy, J. Am. Chem. Soc. 103 (1981) 7176;
(j) J.R. Fox, W.L. Gladfelter, T.G. Wood, J.A. Smegal, T.K. Foreman, G.L. Geoffroy, I. Tavaniepour, V.W. Day, C.S. Day, Inorg. Chem. 20 (1981) 3214;
(k) J.R. Fox, W.L. Gladfelter, G.L. Geoffroy, I. Tavanaiepour, S. Abdel-Mequid, V.W. Day, Inorg. Chem. 20 (1981) 3230;
(l) J.R. Fox, W.L. Gladfelter, G.L. Geoffroy, Inorg. Chem. 19 (1980) 2574.

[7] (a) Some examples S. Yamamoto, K. Asakura, A. Nitta, H. Kuroda, J. Phys. Chem. 96 (1992) 9565;
(b) S. Yamamoto, Y. Miyamoto, R.M. Lewis, M. Koizumi, Y. Morioka, K. Asakura, H. Kuroda, J. Phys. Chem. 96 (1992) 6367;
(c) S. Aime, M. Cisero, R. Gobetto, D. Osella, A. Arce, J. Inorg. Chem. 30 (1991) 1614;
(d) J.R. Budge, B.J. Luecke, B.G. Gates, J. Toran, J. Catal. 91 (1985) 272;
(e) W.A.G. Graham, J.R. Moss, J. Organomet. Chem. 270 (1984) 237;
(f) A. Choplin, M. Leconte, J.M. Basset, S.G. Shore, W.L. Hsu, J. Mol. Catal. 21 (1983) 389;
(g) M.R. Churchill, C. Bueno, W.L. Hsu, J.S. Plotkin, S.G. Shore, Inorg. Chem. 21 (1982) 1958;
(h) J.S. Plotkin, D.G. Alway, C.R. Weisenberger, S.G. Shore, J. Am. Chem. Soc. 102 (1980) 6156.

[8] (a) Examples are: D. Braga, F.Y. Fujiwara, F. Grepioni, R.M.S. Pereira, M.D. Vargas, J. Brazilian Chem. Soc. 10 (1999) 35;
(b) D. Nucciarone, N.J. Taylor, A.J. Carty, Organometallics 7 (1988) 127;
(c) S.A. MacLaughlin, N.J. Taylor, A.J. Carty, Organometallics 3 (1984) 392;
(d) A.J. Carty, S.A. MacLaughlin, N.J. Taylor, J. Organometallic Chem. 204 (1981) C27.

[9] A.G. Orpen, XHYDEX: A Program for Locating Hydrides in Metal Complexes, School of Chemistry, University of Bristol, UK, 1997.

[10] We have previously argued for use of the sum of these bond parameters rather than either of the individual parameters in discussion of metal carbonyls. See, for example W.K. Leong, F.W.B. Einstein, R.K. Pomeroy, J. Cluster Sci. 7 (1996) 121.

[11] W.K. Leong, W.L.J. Leong, J. Zhang, J. Chem. Soc., Dalton Trans. (2001) 1087.

[12] (a) M.I. Bruce, E. Horn, O.B. Shawkataly, M.R. Snow, E.R.T. Tiekink, M.L. Williams, J. Organometallic Chem. 316 (1986) 187;
(b) C. Bergounhou, J.J. Bonnet, P. Fompeyrine, G. Lavigne, N. Lugan, F. Mansilla, Organometallics 5 (1986) 60;
(c) G. Hogarth, J.A. Phillips, F. Van Gastel, N.J. Taylor, T.B. Marder, A.J. Carty, J. Chem. Soc. Chem. Commun. (1988) 1570;
(d) J.F. Corrigan, S. Doherty, N.J. Taylor, A.J. Carty, J. Am. Chem. Soc. 114 (1992) 7557;
(e) J.F. Corrigan, S. Doherty, N.J. Taylor, A.J. Carty, Organometallics 12 (1993) 993;
(f) Y. Chi, A.J. Carty, P. Blenkiron, E. Delgado, G.D. Enright, S.-M. Peng, G.-H. Lee, Organometallics 15 (1996) 5269;
(g) W. Wang, J.F. Corrigan, G.D. Enright, N.J. Taylor, A.J. Carty, Organometallics 17 (1998) 427;
(h) D. Delgado, Y. Chi, W. Wang, G. Hogarth, P.J. Low, G.D. Enright, S.-M. Peng, G.-H. Lee, A.J. Carty, Organometallics 17 (1998) 2936;
(i) G. Süss-Fink, I. Godefroy, A. Béguin, G. Rheinwald, A. Neels, H. Stoeckli-Evans, J. Chem. Soc., Dalton Trans. (1998) 2211.

[13] G. Hogarth, N. Hadj-Bagheri, N.J. Taylor, A.J. Carty, J. Chem. Soc., Chem. Commun. (1990) 1352.

[14] (a) J.R. Fox, W.L. Gladfelter, T.G. Wood, J.A. Smegal, T.K. Foreman, G.L. Geoffroy, I. Tavanaiepour, V.W. Day, C.S. Day, Inorg. Chem. 20 (1981) 3214;
(b) W.L. Gladfelter, G.L. Geoffroy, Inorg. Chem. 19 (1980) 2579.

[15] M.H. Levitt, Spin Dynamics, Wiley, Chichester, 2002.

[16] (a) L.M. Bullock, J.S. Field, R.J. Haines, E. Minshall, M.H. Moore, F. Mulla, D.N. Smit, L.M. Steer, J. Organomet. Chem. 381 (1990) 429;
(b) A.M. Arif, T. Bright, D.E. Heaton, R.A. Jones, C.M. Nunn, Polyhedron 9 (1990) 1573;
(c) V. Patel, A. Cherkas, D. Nucciarone, N.J. Taylor, A.J. Carty, Organometallics 4 (1985) 1793.

[17] J.A. Iggo, NMR Spectroscopy in Inorganic Chemistry, OUP, Oxford, 1999.

[18] L. Pereira, W.K. Leong, S.Y. Wong, J. Organomet. Chem. 609 (2000) 104.

[19] Our study on the disubstituted derivatives have been submitted for publication.

[20] D. Nucciarone, S.A. MacLaughlin, A.J. Carty, Inorg. Synth. 26 (1989) 264.

[21] V.D. Patel, A.A. Cherkas, D. Nucciarone, N.J. Taylor, A.J. Carty, Organometallics 4 (1985) 1792.

[22] (a) A.C. Cooper, K.G. Caulton, Inorg. Chem. 37 (1998) 5938;
(b) L.J. Farrugia, S.E. Rae, Organometallics 10 (1991) 3919;
(c) L.R. Nevinger, J.B. Keister, Organometallics 9 (1990) 2312;
(d) R.F. Alex, R.K. Pomeroy, Organometallics 6 (1987) 2437.

[23] V.D. Bianco, S. Doronzo, Inorg. Synth. 16 (1976) 161.

[24] SMART version 5.628; Bruker AXS Inc.: Madison, Wisconsin, USA, 2001.

[25] SAINT+ version 6.22a; Bruker AXS Inc.: Madison, Wisconsin, USA, 2001.

[26] Sheldrick, G.M. SADABS, 1996.

[27] SHELXTL version 5.1; Bruker AXS Inc.: Madison, Wisconsin, USA, 1997.